Article

Quantum Weighted Fractional-Order Transform

Tieyu Zhao [1,*] and Yingying Chi [2]

[1] Information Science Teaching and Research Section, Northeastern University at Qinhuangdao, Qinhuangdao 066004, China
[2] College of Marxism, Northeastern University at Qinhuangdao, Qinhuangdao 066004, China
* Correspondence: zhaotieyu@neuq.edu.cn

Abstract: Quantum Fourier transform (*QFT*) transformation plays a very important role in the design of many quantum algorithms. Fractional Fourier transform (*FRFT*), as an extension of the Fourier transform, is particularly important due to the design of its quantum algorithm. In this paper, a new reformulation of the weighted fractional Fourier transform (*WFRFT*) is proposed in order to realize quantum *FRFT*; however, we found that this reformulation can be applied to other transformations, and therefore, this paper presents the weighted fractional Hartley transform (*WFRHT*). For the universality of application, we further propose a general weighted fractional-order transform (*WFRT*). When designing the quantum circuits, we realized the quantum *WFRFT* via *QFT* and quantum phase estimation (*QPE*). Moreover, after extending our design to the *WFRHT*, we were able to formulate the quantum *WFRHT*. Finally, in accordance with the research results, we designed the quantum circuit of the general *WFRT*, and subsequently proposed the quantum *WFRT*. The research in this paper has great value as a reference for the design and application of quantum algorithms.

Keywords: quantum fractional Fourier transform; quantum phase estimation; quantum Fourier transform; quantum computation

1. Introduction

The human desire for computing power is endless, and improvements in computing power are closely related to the progress of civilization. Quantum computing comprises parallel computations; this shows that quantum computing quantum algorithms have great advantages over traditional, classical algorithms. Computers are composed of the following four elements: electron tubes, transistors, integrated circuits, and large-scale integrated circuits. As electronic computers continue to develop, chip integration is becoming more common, and a single transistor will eventually be measured on the nanoscopic scale; however, as transistors continue to shrink in size, the physical and chemical properties of the material will qualitatively change, which will lead to the gradual disappearance of the Molar law [1], and the emergence of the quantum effect. Therefore, quantum computing will be important for the next generation of computer research. In 1980, Benioff proposed the quantum Turing machine model, which opened new avenues for quantum computing research [2]. Furthermore, Feynman pointed out that quantum computing has the ability to complete tasks that classical computers cannot [3]. Moreover, the Deutsch–Jozsa algorithm was one of the first to prove the superiority of quantum computing; this algorithm also conceived the physical implementation of the quantum Turing machine and the general quantum computer [4,5]. In 1994, Shor's algorithm was proposed. Shor's algorithm can effectively solve the problem of order finding and factorization using quantum Fourier transform, quantum phase estimation, and other basic operations that involve quantum computing. Compared with classical algorithms, Shor's algorithm can achieve exponential acceleration; undoubtedly, this is a great challenge for public-key cryptography [6]. In 1996, Grover proposed a square root accelerated quantum search algorithm for N unstructured

databases with disordered records [7]. The Grover algorithm aims to use quantum computing technology to solve search problems, and it can achieve square-level acceleration for classical search algorithms. With the introduction of two efficient quantum algorithms, researchers have paid an increasing level of attention to quantum computing; as a result, many improved Grover algorithms appeared [8–12], which has further promoted the development of quantum computing. In addition, applied quantum algorithms have emerged in large numbers; these algorithms are also based on the Grover algorithm [13–18]. In 2009, the emergence of the *HHL* algorithm once again proved the superiority of the quantum algorithm [19], and improvements to the *HHL* algorithm have also been proposed [20–22]. In 2012, Preskill proposed the term "quantum supremacy"; this term highlights that quantum computers may easily answer a class of problems that are complex for classical computers [23]. Moreover, quantum supremacy can be demonstrated on quantum computers using random quantum circuits of more than 50 qubits [24]. A series of quantum computing techniques, such as the quantum Fourier transform (*QFT*) [25], quantum phase estimation (*QPE*) [26], and *HHL* algorithm [19], play a key role in quantum algorithm design; hence, they are called quantum basic linear algebra assemblies [27]. Moreover, these basic operations may be applied to quantum singular value decomposition problems [28] and quantum gradient solving problems [29]. In addition, quantum algorithms play an important role in solving linear equations and differential equations [30–34]. At present, quantum computing has been widely used and it shows great potential.

Out of the abovementioned quantum algorithms, *QFT* and *QPE* play an important role in quantum computing; hence, they are called quantum toolbox algorithms. Similar quantum algorithms include the quantum wavelet transform [35], quantum cosine transform [36], quantum Hartley transform [37], quantum black-box [38,39], and quantum random walk [40,41] algorithms, among others. As an extension of the Fourier transform, fractional Fourier transform (*FRFT*) has a wide range of applications; therefore, the proposal of the quantum fractional Fourier transform (*QFRFT*) is particularly important. Recently, some studies concerning *QFRFT* have been conducted. Unfortunately, these studies do not present a complete quantum circuit [42–45]. Parasa et al. proposed a quantum pseudo-fractional Fourier transform (*QPFRFT*) using multi-valued logic [42]; however, it is not a proper *QFRFT* because it is not unitary. Recently, we presented a *QFRFT* using a quantum artificial neural network, which required using more qubits [46]. There are several diverse definitions of *FRFT* [47,48]. In this paper, the weighted fractional Fourier transform (*WFRFT*) was studied because it is unitary. First, we propose a new reformulation of the *WFRFT*, and we designed its quantum circuit using *QFT* and *QPE*; secondly, we propose a definition for the weighted fractional Hartley transform (*WFRHT*), and the design for the quantum circuit is presented; and finally, the general weighted fractional-order transform (*WFRT*) is defined and the design for its quantum circuit is proposed.

The remainder of this paper is organized as follows. The theories behind *WFRFT*, *WFRHT*, and *WFRT* are analyzed in Section 2. The quantum *WFRFT* is proposed in Section 3. The quantum *WFRHT* is proposed in Section 4. Section 5 discusses the quantum circuit of the *WFRT*. Finally, the conclusions are presented in Section 6.

2. Weighted Fractional-Order Transform

In 1995, the *WFRFT* was proposed [49]. We have studied this algorithm in great detail, and in this paper, we propose a new reformulation of this algorithm; we found that this new reformulation can be used with many new algorithms, such as the *WFRHT*, weighted fractional sine transform (*WFRST*), weighted fractional cosine transform (*WFRCT*), and weighted fractional Hadamard transform (*WFRHaT*) algorithms, among others. Furthermore, we found that when a periodic matrix is given, we can define a new algorithm; thus, we present the definition of the general *WFRT* algorithm in Section 2.3.

2.1. Weighted Fractional Fourier Transform

In 1995, Shih proposed the *WFRFT* using the integer power operation of the Fourier transform [49]. As a generalized version of the Fourier transform, the algorithm can be widely used in signal processing and image encryption, among other fields [50,51]; it is defined as follows:

$$(F^\alpha f)(t) = \sum_{l=0}^{3} A_l^\alpha f_l(t). \tag{1}$$

Here, $f_0(t) = f(t)$, $f_1(t) = (Ff_0)(t)$, $f_2(t) = (Ff_1)(t)$ and $f_3(t) = (Ff_2)(t)$ (F denotes the Fourier transform). The weighting coefficient A_l^α can be expressed as:

$$A_l^\alpha = \cos\left(\frac{(\alpha-l)\pi}{4}\right) \cos\left(\frac{2(\alpha-l)\pi}{4}\right) \exp\left(-\frac{3(\alpha-l)i\pi}{4}\right). \tag{2}$$

For Equation (1), we can also write

$$
\begin{aligned}
F^\alpha[f(t)] &= \sum_{l=0}^{3} A_l^\alpha f_l(t) \\
&= A_0^\alpha f_0(t) + A_1^\alpha f_1(t) + A_2^\alpha f_2(t) + A_3^\alpha f_3(t) \\
&= A_0^\alpha I f(t) + A_1^\alpha F f(t) + A_2^\alpha F^2 f(t) + A_3^\alpha F^3 f(t) \\
&= \left(A_0^\alpha I + A_1^\alpha F + A_2^\alpha F^2 + A_3^\alpha F^3\right) f(t) \\
&= \left(I, F, F^2, F^3\right)
\begin{pmatrix}
A_0^\alpha \\
A_1^\alpha \\
A_2^\alpha \\
A_3^\alpha
\end{pmatrix} f(t).
\end{aligned}
\tag{3}
$$

From [49], we can obtain Equation (4),

$$
\begin{pmatrix}
B_0^\alpha \\
B_1^\alpha \\
B_2^\alpha \\
B_3^\alpha
\end{pmatrix}
=
\begin{pmatrix}
1 & 1 & 1 & 1 \\
1 & i & -1 & -i \\
1 & -1 & 1 & -1 \\
1 & -i & -1 & i
\end{pmatrix}
\begin{pmatrix}
A_0^\alpha \\
A_1^\alpha \\
A_2^\alpha \\
A_3^\alpha
\end{pmatrix},
\tag{4}
$$

where $B_k^\alpha = \exp\left(\frac{2\pi i k\alpha}{4}\right)$; $k = 0, 1, 2, 3$. Via inverse transformation, we can obtain Equation (5),

$$
\begin{pmatrix}
A_0^\alpha \\
A_1^\alpha \\
A_2^\alpha \\
A_3^\alpha
\end{pmatrix}
=
\frac{1}{4}
\begin{pmatrix}
1 & 1 & 1 & 1 \\
1 & -i & -1 & i \\
1 & -1 & 1 & -1 \\
1 & i & -1 & -i
\end{pmatrix}
\begin{pmatrix}
B_0^\alpha \\
B_1^\alpha \\
B_2^\alpha \\
B_3^\alpha
\end{pmatrix}.
\tag{5}
$$

Next, Equation (5) is substituted into Equation (3), so that Equation (6) is obtained.

$$
\begin{aligned}
F^\alpha[f(t)] &= \left(I, F, F^2, F^3\right)
\begin{pmatrix}
A_0^\alpha \\
A_1^\alpha \\
A_2^\alpha \\
A_3^\alpha
\end{pmatrix} f(t) \\
&= \frac{1}{4}\left(I, F, F^2, F^3\right)
\begin{pmatrix}
1 & 1 & 1 & 1 \\
1 & -i & -1 & i \\
1 & -1 & 1 & -1 \\
1 & i & -1 & -i
\end{pmatrix}
\begin{pmatrix}
B_0^\alpha \\
B_1^\alpha \\
B_2^\alpha \\
B_3^\alpha
\end{pmatrix} f(t).
\end{aligned}
\tag{6}
$$

Let

$$
\begin{cases}
Y_0 = I + F + F^2 + F^3 \\
Y_1 = I - iF - F^2 + iF^3 \\
Y_2 = I - F + F^2 - F^3 \\
Y_3 = I + iF - F^2 - iF^3
\end{cases}
\tag{7}
$$

Thus, a new reformulation of *WFRFT* is obtained, as shown in Equation (8).

$$F^\alpha[f(t)] = \frac{1}{4}(Y_0, Y_1, Y_2, Y_3) \begin{pmatrix} B_0^\alpha \\ B_1^\alpha \\ B_2^\alpha \\ B_3^\alpha \end{pmatrix} f(t). \tag{8}$$

Here $B_k^\alpha = \exp\left(\frac{2\pi i k \alpha}{4}\right); k = 0, 1, 2, 3.$

Unitarity is a prerequisite for quantum algorithm design. We can easily prove that the *WFRFT* is unitary using Equation (8) [52]. Moreover, in Section 3, Equation (8) was used to design quantum circuits. The new reformulation that we propose can easily be used with other new algorithms.

2.2. Weighted Fractional Hartley Transform

The abovementioned *WFRFT* uses the Fourier transform as the base function. We know that the discrete Fourier transform (*DFT*) is a periodic matrix with eigenvalues (1, *i*, −1, −*i*). Similar to the *WFRFT*, we can also try to define new fractional-order transforms for other periodic matrices; therefore, we used the Hartley transform as an example. The discrete Hartley transform (*DHT*) has been proposed [53], and its definition is as follows:

$$H = \frac{1}{\sqrt{N}}\left[\cos\left(\frac{2\pi mn}{N}\right) + \sin\left(\frac{2\pi mn}{N}\right)\right]. \tag{9}$$

The *DHT* comprises period **2**; hence, its eigenvalues are 1 and −1. Therefore, we present the definition of *WFRHT* as:

$$(H^\alpha f)(t) = \sum_{l=0}^{1} A_l^\alpha f_l(t). \tag{10}$$

Here, $f_0(t) = f(t)$ and $f_1(t) = (Hf_0)(t)$ (*H* denotes the Hartley transform). The weighting coefficient A_l^α can be obtained using Equation (11),

$$\begin{pmatrix} B_0^\alpha \\ B_1^\alpha \end{pmatrix} = \begin{pmatrix} 1 & 1 \\ 1 & -1 \end{pmatrix}\begin{pmatrix} A_0^\alpha \\ A_1^\alpha \end{pmatrix}, \tag{11}$$

where $B_k^\alpha = \exp(\pi i k \alpha); k = 0, 1.$ Thus, Equation (12) is obtained,

$$\begin{pmatrix} A_0^\alpha \\ A_1^\alpha \end{pmatrix} = \frac{1}{2}\begin{pmatrix} 1 & 1 \\ 1 & -1 \end{pmatrix}\begin{pmatrix} B_0^\alpha \\ B_1^\alpha \end{pmatrix}. \tag{12}$$

Then, Equation (10) can be re-expressed as:

$$\begin{aligned} F^\alpha[f(t)] &= (I, H)\begin{pmatrix} A_0^\alpha \\ A_1^\alpha \end{pmatrix} f(t) \\ &= \frac{1}{2}(I, H)\begin{pmatrix} 1 & 1 \\ 1 & -1 \end{pmatrix}\begin{pmatrix} B_0^\alpha \\ B_1^\alpha \end{pmatrix} f(t). \end{aligned} \tag{13}$$

Let

$$\begin{cases} Y_0 = I + H \\ Y_1 = I - H \end{cases} \tag{14}$$

Therefore, the *WFRHT* can also be expressed as:

$$H^\alpha[f(t)] = \frac{1}{2}(Y_0, Y_1)\begin{pmatrix} B_0^\alpha \\ B_1^\alpha \end{pmatrix} f(t). \tag{15}$$

Here $B_k^\alpha = \exp(\pi i k \alpha); k = 0, 1.$

The discrete sine transform, discrete cosine transform, and discrete Hadamard transform, among other discrete matrices, have period **2**, and their eigenvalues are 1 and -1; therefore, a new algorithm can be defined by replacing the Hartley transform in Equation (14).

2.3. Weighted Fractional-Order Transform

In the analysis of Sections 2.1 and 2.2, it is evident that for periodic transforms (that is, when the matrix of a transform is periodic), we can present the definition of its weighted fractional-order. Next, we present the definition of a general *WFRT*.

Let T denote a periodic matrix (strictly speaking, the matrix should be symmetrical) and $T^M = I$ (M is the period of the matrix T, and I denotes the identity matrix); therefore, the *WFRT* can be defined as:

$$(T^\alpha f)(t) = \sum_{l=0}^{M-1} A_l^\alpha f_l(t).$$ (16)

Here, $f_l(t) = T^l(f(t))$; $l = 0, 1, \cdots, M-1$. The weighting coefficient A_l^α can be obtained by Equation (17),

$$
\begin{pmatrix} B_0^\alpha \\ B_1^\alpha \\ \vdots \\ B_{M-1}^\alpha \end{pmatrix} =
\begin{pmatrix}
w^{0\times 0} & w^{0\times 1} & \cdots & w^{0\times(M-1)} \\
w^{1\times 0} & w^{1\times 1} & \cdots & w^{1\times(M-1)} \\
\vdots & \vdots & \ddots & \vdots \\
w^{(M-1)\times 0} & w^{(M-1)\times 1} & \cdots & w^{(M-1)\times(M-1)}
\end{pmatrix}
\begin{pmatrix} A_0^\alpha \\ A_1^\alpha \\ \vdots \\ A_{M-1}^\alpha \end{pmatrix},
$$ (17)

where $w = e^{2\pi i/M}$ and $B_k^\alpha = e^{2\pi i\alpha k/M}$; $k = 0, 1, \cdots, M-1$. Furthermore, we can obtain Equation (18) as follows:

$$
\begin{pmatrix} A_0^\alpha \\ A_1^\alpha \\ \vdots \\ A_{M-1}^\alpha \end{pmatrix} = \frac{1}{M}
\begin{pmatrix}
u^{0\times 0} & u^{0\times 1} & \cdots & u^{0\times(M-1)} \\
u^{1\times 0} & u^{1\times 1} & \cdots & u^{1\times(M-1)} \\
\vdots & \vdots & \ddots & \vdots \\
u^{(M-1)\times 0} & u^{(M-1)\times 1} & \cdots & u^{(M-1)\times(M-1)}
\end{pmatrix}
\begin{pmatrix} B_0^\alpha \\ B_1^\alpha \\ \vdots \\ B_{M-1}^\alpha \end{pmatrix},
$$ (18)

where $u = e^{-2\pi i/M}$. Next, Equation (16) can be re-expressed as:

$$
\begin{aligned}
(T^\alpha f)(t) &= \sum_{l=0}^{M-1} A_l^\alpha f_l(t) \\
&= \left(I, T, \cdots, T^{M-1} \right)
\begin{pmatrix} A_0^\alpha \\ A_1^\alpha \\ \vdots \\ A_{M-1}^\alpha \end{pmatrix} f(t).
\end{aligned}
$$ (19)

Substituting Equation (18) into Equation (19), we can obtain

$$
\begin{aligned}
(T^\alpha f)(t) &= \sum_{l=0}^{M-1} A_l^\alpha f_l(t) \\
&= \frac{1}{M} \left(I, T, \cdots, T^{M-1} \right)
\begin{pmatrix}
u^{0\times 0} & u^{0\times 1} & \cdots & u^{0\times(M-1)} \\
u^{1\times 0} & u^{1\times 1} & \cdots & u^{1\times(M-1)} \\
\vdots & \vdots & \ddots & \vdots \\
u^{(M-1)\times 0} & u^{(M-1)\times 1} & \cdots & u^{(M-1)\times(M-1)}
\end{pmatrix}
\begin{pmatrix} B_0^\alpha \\ B_1^\alpha \\ \vdots \\ B_{M-1}^\alpha \end{pmatrix} f(t).
\end{aligned}
$$ (20)

Let

$$
\begin{cases}
Y_0 = u^{0 \times 0}I + u^{1 \times 0}T + \cdots + u^{(M-1) \times 0}T^{M-1} \\
Y_1 = u^{0 \times 1}I + u^{1 \times 1}T + \cdots + u^{(M-1) \times 1}T^{M-1} \\
Y_2 = u^{0 \times 2}I + u^{1 \times 2}T + \cdots + u^{(M-1) \times 2}T^{M-1} \\
\quad\vdots \\
Y_{M-1} = u^{0 \times (M-1)}I + u^{1 \times (M-1)}T + \cdots + u^{(M-1) \times (M-1)}T^{M-1}
\end{cases}
\tag{21}
$$

Therefore, the *WFRT* can also be expressed as:

$$
\begin{aligned}
(T^\alpha f)(t) \quad &= \sum_{l=0}^{M-1} A_l^\alpha f_l(t) \\
&= \frac{1}{M}(Y_0, Y_1, \cdots, Y_{M-1})
\begin{pmatrix}
B_0^\alpha \\
B_1^\alpha \\
\vdots \\
B_{M-1}^\alpha
\end{pmatrix}
f(t) \\
&= \frac{1}{M} \sum_{k=0}^{M-1} Y_k B_k^\alpha f(t).
\end{aligned}
\tag{22}
$$

Here $B_k^\alpha = e^{2\pi i \alpha k / M}$ and the *WFRT* is proposed; thus, the *WFRFT* and the *WFRHT* presented above are its special cases. For example, $M = 4$, and T denotes the Fourier transform in Equation (21), which is defined as the *WFRFT*. If $M = 2$, T denotes the Hartley transform in Equation (21), which is the *WFRHT*. This new reformulation can be acceptably applied to the fractional-order definition of periodic functions. Our findings have important value as they can be used as a reference for future information processing and quantum algorithm designs. With increasing demand for greater computing power, we will eventually enter the quantum age. Next, we designed quantum circuits for these algorithms.

3. Quantum Weighted Fractional Fourier Transform

Recently, studies concerning *QFRFT* have been conducted [42–45]; however, these research methods describe the *QFRFT* from the perspective of quantum mechanics, and they do not mention quantum circuits. *FRFT* definitions are diverse, and some definitions are not unitary [47,48]; this causes issues when designing the *QFRFT*. As a result of such difficulties, Parasa et al. showed that *QFRFT* cannot be realized [42]. Recently, we proposed a method to help realize the *QFRFT* using a quantum artificial neural network; however, this method uses more qubits, and thus, it requires more resources [46]. In this section, we will use *QFT* and *QPE* to redesign the *QFRFT* quantum circuit. Studies by Gidney et al. assisted with our research, as follows [54,55].

First, we used *QPE* to obtain the eigenvalues of Equation (7), and the quantum circuit of Equation (7) is shown in Figure 1. The upper part represents the control register, the lower part represents the target register, and $|u\rangle$ represents the feature vector that corresponds with the operator in the target register. Here, we used *QFT* instead of the inverse quantum Fourier transform (*IQFT*) in the control register, as the purpose of this design is to obtain the same results as Equation (7).

From Figure 1, we know

$$
|\psi_0\rangle = |0\rangle \otimes |0\rangle \otimes |u\rangle.
\tag{23}
$$

Via the *H* gate, we obtain

$$
\begin{aligned}
|\psi_1\rangle &= \frac{1}{\sqrt{2}}(|0\rangle + |1\rangle) \otimes \frac{1}{\sqrt{2}}(|0\rangle + |1\rangle) \otimes |u\rangle \\
&= \frac{1}{2}(|00\rangle + |01\rangle + |10\rangle + |11\rangle) \otimes |u\rangle.
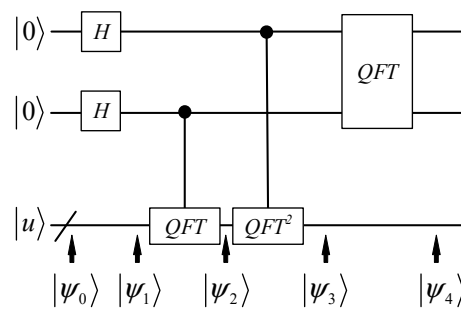\end{aligned}
\tag{24}
$$

Figure 1. The *QPE* for Equation (7).

Then, the *QFT* operation of the target register is,

$$|\psi_2\rangle = \frac{1}{2}(|00\rangle|u\rangle + |01\rangle F|u\rangle + |10\rangle|u\rangle + |11\rangle F|u\rangle), \tag{25}$$

and

$$|\psi_3\rangle = \frac{1}{2}\Big(|00\rangle I|u\rangle + |01\rangle F|u\rangle + |10\rangle F^2|u\rangle + |11\rangle F^3|u\rangle\Big). \tag{26}$$

Here, $|u\rangle$ is the eigenvector of Fourier transform; therefore, $F|u\rangle = D|u\rangle$ (D is the eigenvalue of Fourier transform). The eigenvalue D can be expressed as:

$$D = \begin{pmatrix} \lambda_0 & & & 0 \\ & \lambda_1 & & \\ & & \ddots & \\ 0 & & & \lambda_{n-1} \end{pmatrix}, \tag{27}$$

where $\lambda_j \in \{1, i, -1, -i\}; j = 0, 1, \cdots, n-1$. Therefore, Equation (26) can be expressed as:

$$|\psi_3\rangle = \frac{1}{2}\Big(D^0|00\rangle + D^1|01\rangle + D^2|10\rangle + D^3|11\rangle\Big) \otimes |u\rangle. \tag{28}$$

The eigenvector $|u\rangle$ can be written in accordance with standard orthogonal basis conditions, as shown in Equation (29),

$$|u\rangle = \sum_j b_j |u_j\rangle, \tag{29}$$

where b_j is the projection length. Thus, we can obtain

$$D|u\rangle = \sum_j \lambda_j b_j |u_j\rangle. \tag{30}$$

Equation (28) can be expressed as:

$$|\psi_3\rangle = \frac{1}{2}\left(\sum_j \lambda_j^0 b_j |u_j\rangle|00\rangle + \sum_j \lambda_j^1 b_j |u_j\rangle|01\rangle + \sum_j \lambda_j^2 b_j |u_j\rangle|10\rangle + \sum_j \lambda_j^3 b_j |u_j\rangle|11\rangle\right). \tag{31}$$

The two-qubit *QFT* is used in the control register, and its matrix can be expressed as:

$$QFT = \frac{1}{\sqrt{4}}\begin{pmatrix} 1 & 1 & 1 & 1 \\ 1 & -i & -1 & i \\ 1 & -1 & 1 & -1 \\ 1 & i & -1 & -i \end{pmatrix}. \tag{32}$$

Therefore, we can obtain the following quantum state $|\psi_4\rangle$,

$$|\psi_4\rangle = \sum_j |\phi_j\rangle \otimes b_j |u_j\rangle, \tag{33}$$

where $|\phi_j\rangle \in \{|00\rangle, |01\rangle, |10\rangle, |11\rangle\}$; the results are shown in Figure 2.
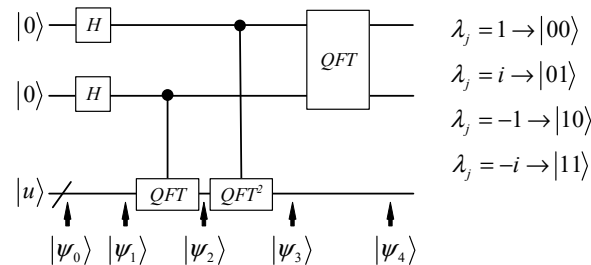
Figure 2. Quantum states corresponding with eigenvalues.

Here, we analyzed the evolutionary process of $|\phi_3\rangle$ to $|\phi_4\rangle$ in detail. Equations (28) and (31) are equivalent; therefore, we can continue to use Equation (28). Then, after the application of the two-qubit QFT, we can obtain

$$|\psi_4\rangle = \frac{1}{4}(W_0|00\rangle + W_1|01\rangle + W_2|10\rangle + W_3|11\rangle) \otimes |u\rangle, \tag{34}$$

where

$$\begin{cases} W_0 = D^0 + D^1 + D^2 + D^3 \\ W_1 = D^0 - iD^1 - D^2 + iD^3 \\ W_2 = D^0 - D^1 + D^2 - D^3 \\ W_3 = D^0 + iD^1 - D^2 - iD^3 \end{cases} \tag{35}$$

Equation (35) is consistent with Equation (7); however, we used the description of the eigenvalues in Equation (7). Furthermore, we know that

$$\begin{aligned} W_0 &= D^0 + D^1 - D^2 + D^3 \\ &= \begin{pmatrix} \lambda_0^0 + i\lambda_0^1 + \lambda_0^2 + \lambda_0^3 & & & \\ & \lambda_1^0 + \lambda_1^1 + \lambda_1^2 + \lambda_1^3 & & \\ & & \ddots & \\ & & & \lambda_{n-1}^0 + \lambda_{n-1}^1 + \lambda_{n-1}^2 + \lambda_{n-1}^3 \end{pmatrix}, \end{aligned} \tag{36}$$

When $\lambda_j = i$,

$$\lambda_j^0 + \lambda_j^1 + \lambda_j^2 + \lambda_j^3 = 0. \tag{38}$$

When $\lambda_j = -1$,

$$\lambda_j^0 + \lambda_j^1 + \lambda_j^2 + \lambda_j^3 = 0. \tag{39}$$

When $\lambda_j = -i$,

$$\lambda_j^0 + \lambda_j^1 + \lambda_j^2 + \lambda_j^3 = 0. \tag{40}$$

Regarding W_0, only in the following circumstance, when $\lambda_j = 1$, is the corresponding element not zero; notably, the elements at the other positions are zero. For W_1,

$$\begin{aligned} W_1 &= D^0 - iD^1 - D^2 + iD^3 \\ &= \begin{pmatrix} \lambda_0^0 - i\lambda_0^1 - \lambda_0^2 + i\lambda_0^3 & & & \\ & \lambda_1^0 - i\lambda_1^1 - \lambda_1^2 + i\lambda_1^3 & & \\ & & \ddots & \\ & & & \lambda_{n-1}^0 - i\lambda_{n-1}^1 - \lambda_{n-1}^2 + i\lambda_{n-1}^3 \end{pmatrix}. \end{aligned} \tag{41}$$

When $\lambda_j = i$,

$$\lambda_j^0 - i\lambda_j^1 - \lambda_j^2 + i\lambda_j^3 = 4. \tag{42}$$

When $\lambda_j = 1, -1, -i$,

$$\lambda_j^0 - i\lambda_j^1 - \lambda_j^2 + i\lambda_j^3 = 0. \tag{43}$$

For W_2,

$$
\begin{aligned}
W_2 &= D^0 - D^1 + D^2 - D^3 \\
&= \begin{pmatrix}
\lambda_0^0 - \lambda_0^1 + \lambda_0^2 - \lambda_0^3 & & & \\
& \lambda_1^0 - \lambda_1^1 + \lambda_1^2 - \lambda_1^3 & & \\
& & \ddots & \\
& & & \lambda_{n-1}^0 - \lambda_{n-1}^1 + \lambda_{n-1}^2 - \lambda_{n-1}^3
\end{pmatrix}.
\end{aligned} \tag{44}
$$

When $\lambda_j = -1$,

$$\lambda_j^0 - \lambda_j^1 + \lambda_j^2 - \lambda_j^3 = 4. \tag{45}$$

When $\lambda_j = 1, i, -i$,

$$\lambda_j^0 - \lambda_j^1 + \lambda_j^2 - \lambda_j^3 = 0. \tag{46}$$

For W_3,

$$
\begin{aligned}
W_3 &= D^0 + iD^1 - D^2 - iD^3 \\
&= \begin{pmatrix}
\lambda_0^0 + i\lambda_0^1 - \lambda_0^2 - i\lambda_0^3 & & & \\
& \lambda_1^0 + i\lambda_1^1 - \lambda_1^2 - i\lambda_1^3 & & \\
& & \ddots & \\
& & & \lambda_{n-1}^0 + i\lambda_{n-1}^1 - \lambda_{n-1}^2 - i\lambda_{n-1}^3
\end{pmatrix}.
\end{aligned} \tag{47}
$$

When $\lambda_j = -i$,

$$\lambda_j^0 + i\lambda_j^1 - \lambda_j^2 - i\lambda_j^3 = 4. \tag{48}$$

When $\lambda_j = 1, i, -1$,

$$\lambda_j^0 + i\lambda_j^1 - \lambda_j^2 - i\lambda_j^3 = 0. \tag{49}$$

Therefore, in Equation (34), we know that for W_0, only in the following circumstance, when the eigenvalue is 1, is the corresponding element not zero. For W_1, W_2, and W_3, the corresponding elements are not zero when the eigenvalues are i, -1, and $-i$, respectively. The number of eigenvalues is shown in Table 1 [56,57]. Then, the combined eigenvectors of W_0, W_1, W_2, and W_3 comprise the exact eigenvectors of the *DFT*. It is evident that Equations (33) and (34) are equivalent.

Table 1. Multiplicities of the *DFT* eigenvalues.

N	**1**	-1	$-i$	i
4n	$n+1$	n	n	$n-1$
$4n+1$	$n+1$	n	n	n
$4n+2$	$n+1$	$n+1$	n	n
$4n+3$	$n+1$	$n+1$	$n+1$	n

Next, we introduced two phase gates (Equations (50) and (51)) and added them to the control register, as shown in Figure 3.
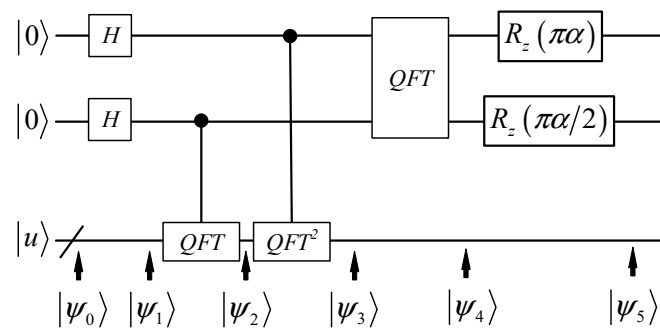
Figure 3. Phase gates are added.

The phase gates $R_Z(\pi\alpha)$ and $R_Z(\pi\alpha/2)$ are expressed as:

$$R_Z(\pi\alpha) = \begin{pmatrix} 1 & 0 \\ 0 & e^{\pi i\alpha} \end{pmatrix},$$ (50)

and

$$R_Z(\pi\alpha/2) = \begin{pmatrix} 1 & 0 \\ 0 & e^{\pi i\alpha/2} \end{pmatrix}.$$ (51)

Thus, we can obtain

$$\begin{pmatrix} 1 & 0 \\ 0 & e^{\pi i\alpha} \end{pmatrix} \otimes \begin{pmatrix} 1 & 0 \\ 0 & e^{\pi i\alpha/2} \end{pmatrix} = \begin{pmatrix} 1 & & & 0 \\ & e^{\pi i\alpha/2} & & \\ & & e^{2\pi i\alpha/2} & \\ 0 & & & e^{3\pi i\alpha/2} \end{pmatrix}.$$ (52)

The diagonal element of the matrix is exactly B_k^α of Equation (8). Then, $|\psi_5\rangle$ is obtained

$$|\psi_5\rangle = \sum_j e^{\pi i\alpha\phi_j/2}|\phi_j\rangle \otimes b_j|u_j\rangle,$$ (53)

where $\phi_j \in \{0,1,2,3\}$ and $|\phi_j\rangle \in \{|00\rangle, |01\rangle, |10\rangle, |11\rangle\}$. Next, we used inverse quantum phase estimation (*IQPE*), as shown in Figure 4.
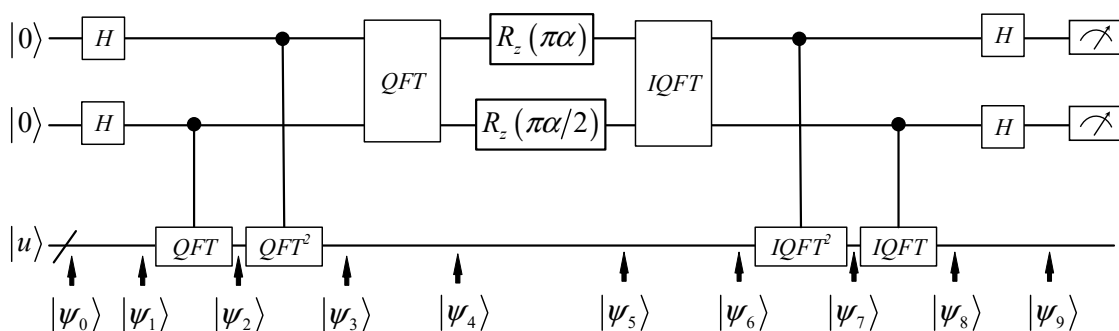

Figure 4. Circuit of the QWFRFT.

The two-qubit *IQFT* of the control register can be expressed as:

$$IQFT = \frac{1}{\sqrt{4}} \begin{pmatrix} 1 & 1 & 1 & 1 \\ 1 & i & -1 & -i \\ 1 & -1 & 1 & -1 \\ 1 & -i & -1 & i \end{pmatrix}.$$ (54)

After the *IQFT* of $|\phi_j\rangle$ is calculated, the eigenvalues are restored,

$$|\psi_6\rangle \quad = \frac{1}{2}\left(\sum_j e^{\pi i \alpha \phi_j/2}\lambda_j^0 b_j |u_j\rangle |00\rangle + \sum_j e^{\pi i \alpha \phi_j/2}\lambda_j^1 b_j |u_j\rangle |01\rangle + \sum_j e^{\pi i \alpha \phi_j/2}\lambda_j^2 b_j |u_j\rangle |10\rangle + \sum_j e^{\pi i \alpha \phi_j/2}\lambda_j^3 b_j |u_j\rangle |11\rangle\right)$$

$$= \frac{1}{2}\left(\sum_j e^{\pi i \alpha \phi_j/2} b_j |u_j\rangle |00\rangle + \sum_j e^{\pi i \alpha \phi_j/2} F b_j |u_j\rangle |01\rangle + \sum_j e^{\pi i \alpha \phi_j/2} F^2 b_j |u_j\rangle |10\rangle + \sum_j e^{\pi i \alpha \phi_j/2} F^3 b_j |u_j\rangle |11\rangle\right). \tag{55}$$

Next,

$$|\psi_7\rangle = \frac{1}{2}\left(\sum_j e^{\pi i \alpha \phi_j/2}\lambda_j^0 a_j |u_j\rangle |00\rangle + \sum_j e^{\pi i \alpha \phi_j/2} F b_j |u_j\rangle |01\rangle + \sum_j e^{\pi i \alpha \phi_j/2} IF^2 F^2 b_j |u_j\rangle |10\rangle + \sum_j e^{\pi i \alpha \phi_j/2} IF^2 F^3 b_j |u_j\rangle |11\rangle\right), \tag{56}$$

where *IF* denotes the inverse Fourier transform.

$$|\psi_8\rangle \quad = \frac{1}{2}\left(\sum_j e^{\pi i \alpha \phi_j/2}\lambda_j^0 b_j |u_j\rangle |00\rangle + \sum_j e^{\pi i \alpha \phi_j/2} IFF b_j |u_j\rangle |01\rangle + \sum_j e^{\pi i \alpha \phi_j/2} IF^2 F^2 b_j |u_j\rangle |10\rangle + \sum_j e^{\pi i \alpha \phi_j/2} IF^3 F^3 b_j |u_j\rangle |11\rangle\right)$$

$$= \frac{1}{2}\left(\sum_j e^{\pi i \alpha \phi_j/2} b_j |u_j\rangle |00\rangle + \sum_j e^{\pi i \alpha \phi_j/2} b_j |u_j\rangle |01\rangle + \sum_j e^{\pi i \alpha \phi_j/2} b_j |u_j\rangle |10\rangle + \sum_j e^{\pi i \alpha \phi_j/2} b_j |u_j\rangle |11\rangle\right) \tag{57}$$

$$= \sum_j e^{\pi i \alpha \phi_j/2} b_j |u_j\rangle \frac{1}{\sqrt{2}}(|0\rangle + |1\rangle)\frac{1}{\sqrt{2}}(|0\rangle + |1\rangle).$$

Finally, through the *H* gate, we obtain $|\psi_9\rangle$

$$|\psi_9\rangle = |0\rangle |0\rangle \sum_j e^{\pi i \alpha \phi_j/2} b_j |u_j\rangle, \tag{58}$$

where $\phi_j \in \{0,1,2,3\}$. We know

$$\sum_j e^{\pi i \phi_j/2} b_j |u_j\rangle = F|u\rangle, \tag{59}$$

so

$$\sum_j e^{\pi i \alpha \phi_j/2} b_j |u_j\rangle = F^\alpha |u\rangle. \tag{60}$$

Then, Equation (58) is expressed as:

$$|\psi_9\rangle = |0\rangle |0\rangle F^\alpha |u\rangle. \tag{61}$$

Therefore, the quantum *WFRFT* (*QWFRFT*) is obtained.

The *QWFRFT* was designed as shown in Figure 4. This design provides the foundation for subsequent quantum *WFRHT* designs (*QWFRHT*).

4. Quantum Weighted Fractional Hartley Transform

The quantum Hartley transform (*QHT*) has been proposed [37]. Next, we use *QPE* and *QHT* to design the circuit of the *QWFRHT*, as shown in Figure 5. The eigenvalues of the Hartley transform are 1 and −1; therefore, the control register only needs one qubit to complete the circuit.
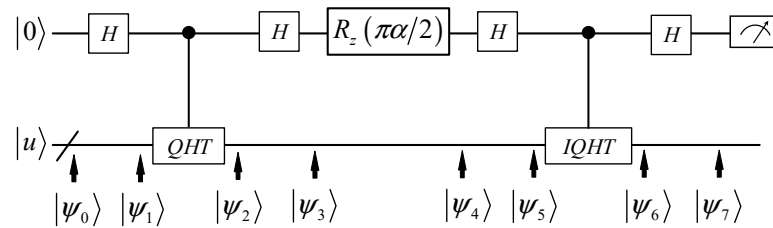
Figure 5. The *QWFRHT* circuit.

Here, $|u\rangle$ is the eigenvector of the Hartley transform; thus, we can obtain

$$|\psi_0\rangle = |0\rangle \otimes |u\rangle, \tag{62}$$

$$|\psi_1\rangle = \frac{1}{\sqrt{2}}(|0\rangle + |1\rangle) \otimes |u\rangle, \tag{63}$$

and

$$\begin{aligned}|\psi_2\rangle &= \frac{1}{\sqrt{2}}(I|0\rangle|u\rangle + QHT|1\rangle|u\rangle) \\ &= \frac{1}{\sqrt{2}}(D^0|0\rangle + D|1\rangle) \otimes |u\rangle.\end{aligned} \tag{64}$$

We know $QHT|u\rangle = D|u\rangle$. Here, D is the eigenvalue of the Hartley transform and it can be expressed as:

$$D = \begin{pmatrix} \lambda_0 & & & 0 \\ & \lambda_1 & & \\ & & \ddots & \\ 0 & & & \lambda_{n-1} \end{pmatrix}, \tag{65}$$

where $\lambda_j \in \{1, -1\}; j = 0, 1, \cdots, n-1$. This is because

$$|u\rangle = \sum_j r_j |u_j\rangle, \tag{66}$$

therefore,

$$D|u\rangle = \sum_j \lambda_j r_j |u_j\rangle. \tag{67}$$

Equation (64) can be expressed as:

$$|\psi_2\rangle = \frac{1}{\sqrt{2}} \left(\sum_j \lambda_j^0 r_j |u_j\rangle|0\rangle + \sum_j \lambda_j^1 r_j |u_j\rangle|1\rangle \right). \tag{68}$$

Similarly to the abovementioned *QWFRFT*, after passing through the *H* gate, we obtain

$$|\psi_3\rangle = \sum_j |\phi_j\rangle \otimes r_j |u_j\rangle, \tag{69}$$

where $|\phi_j\rangle \in \{|0\rangle, |1\rangle\}$; thus, the phase gate of Equation (50) is used,

$$|\psi_4\rangle = \sum_j e^{\pi i \alpha \phi_j} |\phi_j\rangle \otimes r_j |u_j\rangle. \tag{70}$$

Next, the *IQPE* is used, so that the eigenvalues can be recovered:

$$|\psi_5\rangle = \frac{1}{\sqrt{2}} \left(\sum_j e^{\pi i \alpha \phi_j} \lambda_j^0 r_j |u_j\rangle|0\rangle + \sum_j e^{\pi i \alpha \phi_j} \lambda_j^1 r_j |u_j\rangle|1\rangle \right), \tag{71}$$

and

$$|\psi_6\rangle = \frac{1}{\sqrt{2}}\left(\sum_j e^{\pi i\alpha]\phi_j} r_j|u_j\rangle|0\rangle + \sum_j e^{\pi i\alpha\phi_j} r_j|u_j\rangle|1\rangle\right)$$
$$= \sum_j e^{\pi i\alpha\phi_j} r_j|u_j\rangle\frac{1}{\sqrt{2}}(|0\rangle + |1\rangle). \tag{72}$$

Finally, we obtain

$$|\psi_7\rangle = |0\rangle\sum_j e^{\pi i\alpha\phi_j} r_j|u_j\rangle. \tag{73}$$

This is because

$$\sum_j e^{\pi i]\phi_j} r_j|u_j\rangle = H|u\rangle, \tag{74}$$

where H denotes the Hartley transform; therefore,

$$\sum_j e^{\pi i\alpha\phi_j} r_j|u_j\rangle = H^\alpha|u\rangle. \tag{75}$$

Then, Equation (73) is expressed as

$$|\psi_7\rangle = |0\rangle H^\alpha|u\rangle. \tag{76}$$

Thus, the *QWFRHT* is obtained.

Similarly to the *QWFRHT*, the quantum sine transform, quantum Hadamard transform, quantum cosine transform, and so on, are periodic functions, and their eigenvalues are 1 and −1; therefore, the designs of these functions are consistent with the findings in this section.

5. Discussion

With the help of the designs in Sections 3 and 4, in this section, we present the quantum circuit of the *WFRT* (*QWFRT*); that is, the quantum circuit design of the *WFRT* in Section 2.3. Moreover, in this section, the unitary matrix $T^M = I$ (M is the period and I is the identity matrix) is determined. In order to fulfil the design requirements, the period should satisfy $M = 2^q$. We also used *QPE* to design quantum circuits, as shown in Figure 6.
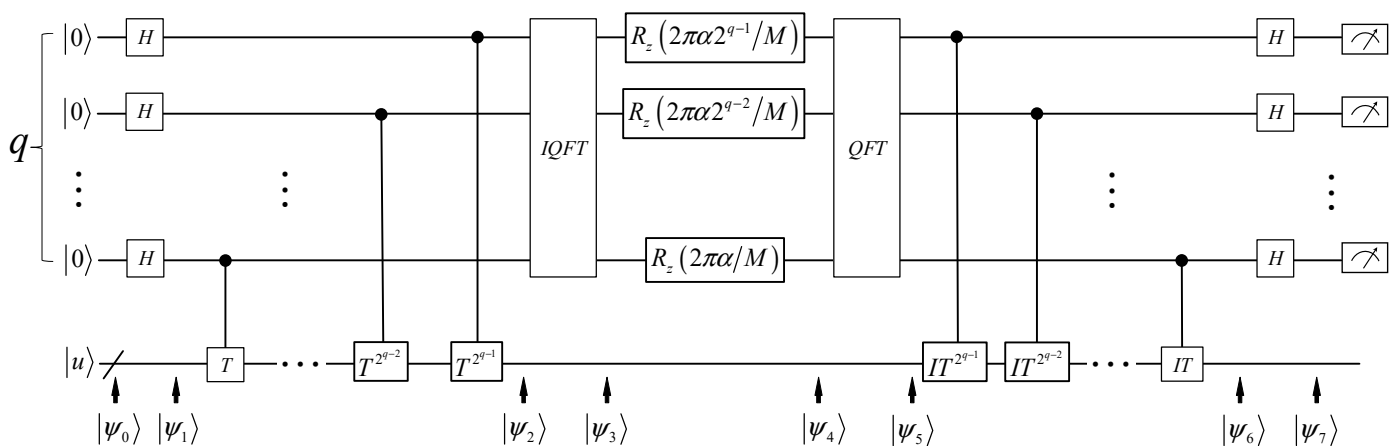

Figure 6. The circuit of *QWFRT*.

Here, $|u\rangle$ is the eigenvector of matrix T; thus, we can obtain

$$|\psi_0\rangle = |0\rangle^{\otimes q}|u\rangle, \tag{77}$$

where $q = \log_2^M$. Thus

$$|\psi_1\rangle = \frac{1}{\sqrt{2^q}}(|0\rangle + |1\rangle)^{\otimes q}|u\rangle, \tag{78}$$

and

$$|\psi_2\rangle = \frac{1}{\sqrt{2^q}}\left(|0\rangle + T^{2^{q-1}}|1\rangle\right)\left(|0\rangle + T^{2^{q-2}}|1\rangle\right) \otimes \cdots \otimes (|0\rangle + T|1\rangle) \otimes |u\rangle. \tag{79}$$

This is because $M = 2^q$ and $|u\rangle = \sum_j c_j|u_j\rangle$; therefore, Equation (79) can be expressed as:

$$\begin{aligned}|\psi_2\rangle &= \frac{1}{\sqrt{2^q}}\sum_{k=0}^{M-1}|k\rangle T^k|u\rangle \\ &= \frac{1}{\sqrt{2^q}}\sum_{k=0}^{M-1}|k\rangle\sum_j \lambda_j^k c_j|u_j\rangle.\end{aligned} \tag{80}$$

Then, after the q-qubit *IQFT* of $\sum\limits_{k=0}^{M-1}\lambda_j^k|k\rangle$, we obtain

$$|\psi_3\rangle = \sum_j |\phi_j\rangle c_j|u_j\rangle. \tag{81}$$

Via the phase gates, we can obtain

$$|\psi_4\rangle = \sum_j e^{2\pi i\alpha\phi_j/M}|\phi_j\rangle c_j|u_j\rangle. \tag{82}$$

Next, the *IQPE* is used. First, for the q-qubit *QFT* of $|\phi_j\rangle$, the eigenvalues are recovered,

$$|\psi_5\rangle = \frac{1}{\sqrt{2^q}}\sum_j e^{2\pi i\alpha\phi_j/M}\sum_{k=0}^{M-1}\lambda_j^k|k\rangle c_j|u_j\rangle. \tag{83}$$

Hence,

$$|\psi_6\rangle = \frac{1}{\sqrt{2^q}}\sum_j e^{2\pi i\alpha\phi_j/M}\sum_{k=0}^{M-1}|k\rangle c_j|u_j\rangle. \tag{84}$$

where $\phi_j \in (0, 1, \cdots, M-1)$. Finally, we obtain

$$|\psi_7\rangle = |0\rangle^{\otimes q}\sum_j e^{2\pi i\alpha\phi_j/M}c_j|u_j\rangle. \tag{85}$$

Thus

$$|\psi_7\rangle = |0\rangle^{\otimes q}T^\alpha|u\rangle. \tag{86}$$

Ergo, the *QWFRT* is obtained.

In the quantum circuit of Figure 6, the upper part represents the control register, and the lower part represents the target register. The quantum bits required in the control register are closely related to the period of the unitary matrix T, which is $q = \log_2^M$. In the quantum circuit of Figure 4, the period of the Fourier transform is 4; that is, $M = 4$; therefore, in the circuit design, the control register needs two qubits. Similarly, in the quantum circuit of Figure 5, the period of the Hartley transform is 2; that is, $M = 2$; therefore, we used a qubit in the control register. Therefore, it is evident that the schemes proposed in Sections 3 and 4 are special cases of the scheme proposed in Section 5.

Due to the complexity of the designed quantum algorithm, in space, in order to store eigenvalues, we use an additional q qubits (control registers). The qubits required for the control registers of different algorithms may also be different. For example, for the *QWFRFT* in Figure 4, we use two auxiliary qubits to store eigenvalues; for the *QWFRHT* in Figure 5, we use only one auxiliary qubit to store the eigenvalues. That is to say, the qubit

of the control register depends on the number of eigenvalues of the algorithm. In time, when the target register is large, we only consider the complexity of the quantum gate in the circuit. Taking the *QWFRFT* in Figure 4 as an example, we use three *QFT*s and three *IQFT*s, and the complexity of each *QFT* and *IQFT* is $O(n^2)$. Therefore, the time complexity of the *QWFRT* depends on the complexity of quantum algorithm *T*.

6. Conclusions

As a generalized Fourier transform algorithm, the quantum circuit design of *FRFT* is particularly important. In order to design a *QFRFT*, we first analyzed the definitions for *WFRFT*; then, we proposed a new reformulation. Based on the new reformulation, we presented the *WFRHT*, and this fractional-order definition may also be applicable to the sine transform, cosine transform, and Hadamard transform algorithms; therefore, we proposed an additional weighted fractional-order definition based on the periodic matrix, which has wide applicability. Moreover, the proposed new reformulation contributes to the design of quantum algorithms. We first used *QFT* and *QPE* to design the quantum circuit of *WFRFT*; then, we designed the *QWFRHT*, a design which has wide applicability. Moreover, by designing the quantum circuit of the *WFRT*, we were able to realize the *QWFRT*. The quantum algorithms proposed in this paper will have great value in terms of their ability to be used as a reference for future quantum information processing.

Institutional Review Board Statement: Not applicable.

Informed Consent Statement: Not applicable.

Data Availability Statement: Not applicable.

Conflicts of Interest: The authors declare no conflict of interest.

References

1. Moore, G.E. *Cramming More Components onto Integrated Circuits*; McGraw-Hill: New York, NY, USA, 1965; Volume 38, pp. 114–117.
2. Benioff, P. The computer as a physical system: A microscopic quantum mechanical Hamiltonian model of computers as represented by Turing machines. *J. Stat. Phys.* **1980**, *22*, 563–591. [CrossRef]
3. Feynman, R.P. Simulating physics with computers. *Int. J. Theor. Phys.* **1982**, *21*, 467–488. [CrossRef]
4. Deutsch, D.; Jozsa, R. Rapid solution of problems by quantum computation. *Proc. R. Soc. Lond. Ser. A Math. Phys. Sci.* **1992**, *439*, 553–558. [CrossRef]
5. Deutsch, D. Quantum theory, the Church–Turing principle and the universal quantum computer. *Proc. R. Soc. Lond. Ser. A Math. Phys. Sci.* **1985**, *400*, 97–117.
6. Shor, P.W. Algorithms for Quantum Computation: Discrete Logarithms and Factoring. In Proceedings of the 35th Annual Symposium on Foundation of Computer Science, Washington, DC, USA, 20–22 November 1994; pp. 124–134.
7. Grover, L.K. A fast quantum mechanical algorithm for database search. In Proceedings of the Twenty-Eighth Annual ACM Symposium on Theory of Computing, Philadelphia, PA, USA, 1 July 1996; pp. 212–219.
8. Boyer, M.; Brassard, G.; Høyer, P.; Tapp, A. Tight bounds on quantum searching. *Fortschr. Phys. Prog. Phys.* **1998**, *46*, 493–505. [CrossRef]
9. Grover, L.K. Quantum Computers Can Search Rapidly by Using Almost Any Transformation. *Phys. Rev. Lett.* **1998**, *80*, 4329–4332. [CrossRef]
10. Biham, E.; Biham, O.; Biron, D.; Grassl, M.; Lidar, D.A. Grover's quantum search algorithm for an arbitrary initial amplitude distribution. *Phys. Rev. A* **1999**, *60*, 2742–2745. [CrossRef]
11. Long, G.L. Grover algorithm with zero theoretical failure rate. *Phys. Rev. A* **2001**, *64*, 022307. [CrossRef]
12. Li, P.; Li, S. Phase matching in Grover's algorithm. *Phys. Lett. A* **2007**, *366*, 42–46. [CrossRef]
13. Brassard, G.; Høyer, P.; Tapp, A. Quantum counting, Automata, Languages and Programming. In Proceedings of the 25th International Colloquium, ICALP'98, Aalborg, Denmark, 13–17 July 1998; Springer: Berlin/Heidelberg, Germany, 1998; pp. 820–831.
14. Grover, L.K. Synthesis of Quantum Superpositions by Quantum Computation. *Phys. Rev. Lett.* **2000**, *85*, 1334–1337. [CrossRef]

15. Hao, G.; Gui-Lu, L.; Feng, L. Quantum Algorithms for Some Well-Known NP Problems. *Commun. Theor. Phys.* **2002**, *37*, 424–426. [CrossRef]
16. Pang, C.-Y.; Zhou, R.-G.; Ding, C.-B.; Hu, B.-Q. Quantum search algorithm for set operation. *Quantum Inf. Process.* **2012**, *12*, 481–492. [CrossRef]
17. Furrow, B. A panoply of quantum algorithms. *arXiv* **2006**, arXiv:quant-ph/0606127. [CrossRef]
18. Baritompa, W.P.; Bulger, D.W.; Wood, G.R. Grover's quantum algorithm applied to global optimization. *SIAM J. Optim.* **2005**, *15*, 1170–1184. [CrossRef]
19. Harrow, A.W.; Hassidim, A.; Lloyd, S. Quantum Algorithm for Linear Systems of Equations. *Phys. Rev. Lett.* **2009**, *103*, 150502. [CrossRef]
20. Clader, B.D.; Jacobs, B.C.; Sprouse, C.R. Preconditioned Quantum Linear System Algorithm. *Phys. Rev. Lett.* **2013**, *110*, 250504. [CrossRef]
21. Childs, R.K.A.M.; Kothari, R.; Somma, R.D. Quantum Algorithm for Systems of Linear Equations with Exponentially Improved Dependence on Precision. *SIAM J. Comput.* **2017**, *46*, 1920–1950. [CrossRef]
22. Wossnig, L.; Zhao, Z.; Prakash, A. Quantum Linear System Algorithm for Dense Matrices. *Phys. Rev. Lett.* **2018**, *120*, 050502. [CrossRef]
23. Preskill, J. Quantum computing and the entanglement frontier. *arXiv* **2012**, arXiv:1203.5813.
24. Boixo, S.; Isakov, S.V.; Smelyanskiy, V.N.; Babbush, R.; Ding, N.; Jiang, Z.; Bremner, M.J.; Martinis, J.M.; Neven, H. Characterizing quantum supremacy in near-term devices. *Nat. Phys.* **2018**, *14*, 595–600. [CrossRef]
25. Coppersmith, D. An approximate Fourier transform useful in quantum factoring. *arXiv* **2002**, arXiv:quant-ph/0201067.
26. Nielsen, M.A.; Chuang, I.L. Quantum computation and quantum information. *Phys. Today* **2001**, *54*, 60. [CrossRef]
27. Biamonte, J.; Wittek, P.; Pancotti, N.; Rebentrost, P.; Wiebe, N.; Lloyd, S. Quantum machine learning. *Nature* **2017**, *549*, 195–202. [CrossRef] [PubMed]
28. Rebentrost, P.; Steffens, A.; Marvian, I.; Lloyd, S. Quantum singular-value decomposition of nonsparse low-rank matrices. *Phys. Rev. A* **2018**, *97*, 012327. [CrossRef]
29. Rebentrost, P.; Schuld, M.; Wossnig, L.; Petruccione, F.; Lloyd, S. Quantum gradient descent and Newton's method for constrained polynomial optimization. *New J. Phys.* **2019**, *21*, 073023. [CrossRef]
30. Higgott, O.; Wang, D.; Brierley, S. Variational Quantum Computation of Excited States. *Quantum* **2019**, *3*, 156. [CrossRef]
31. Bravo-Prieto, C.; Larose, R.; Cerezo, M.; Subasi, Y.; Cincio, L.; Coles, P. Variational Quantum Linear Solver: A Hybrid Algorithm for Linear Systems. *Am. Phys. Soc.* **2020**, *65*, 1.
32. LaRose, R.; Tikku, A.; O'Neel-Judy, É.; Cincio, L.; Coles, P.J. Variational quantum state diagonalization. *NPJ Quantum Inf.* **2019**, *5*, 57. [CrossRef]
33. Arrazola, J.M.; Kalajdzievski, T.; Weedbrook, C.; Lloyd, S. Quantum algorithm for nonhomogeneous linear partial differential equations. *Phys. Rev. A* **2019**, *100*, 032306. [CrossRef]
34. Childs, A.M.; Liu, J.-P. Quantum Spectral Methods for Differential Equations. *Commun. Math. Phys.* **2020**, *375*, 1427–1457. [CrossRef]
35. Fijany, A.; Williams, C.P. Quantum wavelet transforms: Fast algorithms and complete circuits. In Proceedings of the Quantum Computing and Quantum Communications: First NASA International Conference, QCQC'98, Palm Springs, CA, USA, 17–20 February 1998; Springer: Berlin/Heidelberg, Germany, 1999; pp. 10–33.
36. Klappenecker, A.; Rotteler, M. Discrete cosine transforms on quantum computers. In Proceedings of the ISPA 2001. Proceedings of the 2nd International Symposium on Image and Signal Processing and Analysis. In Conjunction with 23rd International Conference on Information Technology Interfaces, Pula, Croatia, 19–21 June 2001; pp. 464–468.
37. Tseng, C.-C.; Hwang, T.-M. Quantum Circuit Design of Discrete Hartley Transform using Recursive Decomposition Formula. In Proceedings of the 2005 IEEE International Symposium on Circuits and Systems (ISCAS), Kobe, Japan, 23–26 May 2005; Volume 1, pp. 824–827. [CrossRef]
38. Mermin, N.D. Quantum mysteries refined. *Am. J. Phys.* **1994**, *62*, 880–887. [CrossRef]
39. Berthiaume, A.; Brassard, G. Oracle Quantum Computing. *J. Mod. Opt.* **1994**, *41*, 2521–2535. [CrossRef]
40. Aharonov, Y.; Davidovich, L.; Zagury, N. Quantum random walks. *Phys. Rev. A* **1993**, *48*, 1687. [CrossRef]
41. Venegas-Andraca, S.E.; Ball, J.L.; Burnett, K.; Bose, S. Quantum walks with entangled coins. *New J. Phys.* **2005**, *7*, 221. [CrossRef]
42. Parasa, V.; Perkowski, M. Quantum Pseudo-Fractional Fourier Transform Using Multiple-Valued Logic. In Proceedings of the 2012 IEEE 42nd International Symposium on Multiple-Valued Logic, Victoria, BC, Canada, 14–16 May 2012; pp. 311–314. [CrossRef]
43. Lv, C.-H.; Fan, H.-Y.; Li, D. From fractional Fourier transformation to quantum mechanical fractional squeezing transformation. *Chin. Phys. B* **2015**, *24*, 020301. [CrossRef]
44. Weimann, S.; Perez-Leija, A.; Lebugle, M.; Keil, R.; Tichy, M.; Gräfe, M.; Heilmann, R.; Nolte, S.; Moya-Cessa, H.; Weihs, G.; et al. Implementation of quantum and classical discrete fractional Fourier transforms. *Nat. Commun.* **2016**, *7*, 11027. [CrossRef] [PubMed]
45. Madrid, Y.; Molina, M.; Torres, R. Quantum Fractional Fourier Transform. In *Frontiers in Optics*; Optica Publishing Group: Washington, DC, USA, 2018.
46. Zhao, T.; Yang, T.; Chi, Y. Quantum Weighted Fractional Fourier Transform. *Mathematics* **2022**, *10*, 1896. [CrossRef]
47. Tao, R.; Zhang, F.; Wang, Y. Research progress on discretization of fractional Fourier transform. *Sci. China Inf. Sci.* **2008**, *51*, 859–880. [CrossRef]
48. Gómez-Echavarría, A.; Ugarte, J.P.; Tobón, C. The fractional Fourier transform as a biomedical signal and image processing tool: A review. *Biocybern. Biomed. Eng.* **2020**, *40*, 1081–1093. [CrossRef]

49. Shih, C.-C. Fractionalization of Fourier transform. *Opt. Commun.* **1995**, *118*, 495–498. [CrossRef]
50. Liang, Y.; Da, X.; Xu, R.; Ni, L.; Zhai, D.; Pan, Y. Research on Constellation-Splitting Criterion in Multiple Parameters WFRFT Modulations. *IEEE Access* **2018**, *6*, 34354–34364. [CrossRef]
51. Zhao, T.; Ran, Q. The Weighted Fractional Fourier Transform and Its Application in Image Encryption. *Math. Probl. Eng.* **2019**, *2019*, 4789194. [CrossRef]
52. Zhao, T.; Chi, Y. Multiweighted-Type Fractional Fourier Transform: Unitarity. *Fractal Fract.* **2021**, *5*, 205. [CrossRef]
53. Bracewell, R.N. Discrete hartley transform. *JOSA* **1983**, *73*, 1832–1835. [CrossRef]
54. Gidney, C. Computing Fractional Fourier Transforms. 2017. Available online: https://algassert.com/post/1710 (accessed on 11 June 2017).
55. Pang, H. Circuit Construction of Quantum Fractional Fourier Transform. *Zhihu*. 2022. Available online: https://zhuanlan.zhihu.com/p/489812535 (accessed on 31 March 2022).
56. McClellan, J.; Parks, T. Eigenvalue and eigenvector decomposition of the discrete Fourier transform. *IEEE Trans. Audio Electroacoust.* **1972**, *20*, 66–74. [CrossRef]
57. Dickinson, B.; Steiglitz, K. Eigenvectors and functions of the discrete Fourier transform. *IEEE Trans. Acoust. Speech Signal Process.* **1982**, *30*, 25–31. [CrossRef]